Gravitationally self-bound quantum states in unstable potentials

Markku Jääskeläinen
Division of Physics and Mathemaics/Natural Sciences with Didactics, Mälardalen University, Box 883, 72123 Västerås, Sweden

(Received 23 November 2017; published 19 April 2018)

Quantum mechanics at present cannot be unified with the theory of gravity at the deepest level, and to guide research towards the solution of this fundamental problem, we need to look for ways to observe or refute predictions originating from attempts to combine quantum theory with gravity. The influence of the gravitational field created by the material density given by the wave function itself gives rise to nontrivial phenomena. In this study I consider the wave function for the center-of-mass coordinate of a spherical mass distribution under the influence of the self-interaction of Newtonian gravity. I solve numerically for the ground state in the presence of an unstable potential and find that the energy of the free-space bound state can be lowered despite the nontrapping character of the potential. The center-of-mass ground state becomes increasingly localized for the used unstable potentials, although only in a limited parameter regime. The feebleness of the energy shift makes the observation of these effects demanding and requires further developments in the cooling of material particles. In addition, the influence of gravitational perturbations that are present in typical laboratory settings necessitates the use of extremely quiet and controlled environments such as those provided by recently proposed space-borne experiments.

DOI: 10.1103/PhysRevA.97.042116

I. INTRODUCTION

For quite some time, uniting quantum mechanics with general relativistic gravity has been a problem at the forefront of physics, and it remains an unsolved problem at the deepest fundamental level [1–3]. Quantum mechanics of objects in an external gravitational field, on the other hand, is unproblematic, and both interference [4] and the effects of transverse bound states have been demonstrated experimentally for neutrons in gravitational fields [5]. Cesium atoms have been sent bouncing multiple times in a stable gravitational cavity [6] experiencing the acceleration due to earth's gravitational field. Atom interferometry has been performed with path separations that are half a meter in size, showing that quantum mechanics of massive, albeit very light, objects applies to macroscopic separations [7].

Moving beyond trivial effects of external fields will require the observation of quantum behavior of larger bodies. One proposed avenue for extending quantum mechanics to solid bodies approaching macroscopic sizes, quantum optomechanics, is a fast-developing field [8] and experiments on massive objects in the quantum regime have been proposed [9,10], some that even include living organisms [11]. These experiments start approaching the traditional quantum-classical boundary [12], and one characteristic of classical bodies is that they are sources of a gravitational field. A framework for uniting quantum mechanics with static Newtonian gravity exists [13,14], and the phenomenology of quantum mechanics of self-gravitating degenerate systems has already been studied theoretically for some time [15]. The detection of self-gravitational effects in quantum systems [16] will have profound influence on physics, even at the interpretational level [17]. It is therefore important to investigate what possible phenomena exist and further to investigate whether or not they are within the reach of present and planned experiments. Quantum descriptions of extended self-gravitating objects raise questions of a fundamental nature, and issues regarding the framework are actively studied [18,19] as are properties of the resulting equation, presently known as the Newton-Schrödinger equation [13,14,20–23]. For a nonrelativistic system under the influence of mutually and self-interacting gravitational fields [13], the state is determined by the stationary Schrödinger equation. In earlier works, the system of a free, self-gravitating spherical mass was shown to have a bound state with two different regimes [20,24].

Here I investigate the effects of adding an external potential to the system and discuss limits for observing them. Earlier studies investigated the effect of self-gravity on the dynamics of squeezed states [22], and energy shifts of bound states of a trapping harmonic potential [21]. The investigations here are done for masses that are low enough to experience quantum effects due to the extended density distribution. In Sec. II the theoretical framework is outlined and in Sec. IV the results of the main studies in this paper are reported. In Sec. V the results of the preceding section as well as conditions needed to observe them are discussed.

II. THEORY

For a homogeneous solid sphere described using quantum mechanics, we expect that the intrinsic position uncertainty of the individual atoms will result in a matter density $\rho_M(\vec{r})$ spread out to a finite spatial extent. In principle, the system is governed by a many-particle wave function describing all the individual particles that constitute the sphere and the resulting dynamics are of a prohibitively high dimension for exact analytical treatments. In practice, a separation into center-of-mass and relative coordinates [17] gives rise to a solution for the former due to the electromagnetic interparticle interaction, the familiar bulk solid. The solid has a characteristic energy far larger than that possible for the remaining center-of-mass problem. This procedure results in the center-of-mass wave function $\Psi(\vec{r})$ being

treated as an independent dynamical entity. Here I will focus on a solid sphere as the material object. Combining the separation procedure with a continuum approximation for the solid density drastically simplifies the treatment, and for the center-of-mass description this leads to appearance of averaged phenomena in the low-energy regime. For instance, a simplified expression for the density distribution is given by

$$\rho_M(\vec{r}) = \rho_0 \int_{\mathbb{R}^3} \Theta(|\vec{r} - \vec{r}\,'| < 2R)|\Psi(\vec{r}\,')|^2 dV', \quad (1)$$

where ρ_0 corresponds to the bulk density determined by the solution for the relative coordinates in the variable separated many-body problem and R is the radius of the solid sphere. This material density has a spread in space due to the position uncertainty of the center-of-mass wave function $\Psi(\vec{r})$. Under reasonable assumptions $\rho_M(\vec{r})$ can be taken to act as a physical source for a gravitational field $U_G(\vec{r})$ [17], which will then be governed by a Poisson equation

$$\nabla^2 U_G(\vec{r}) = -4\pi G \rho_M(\vec{r}). \quad (2)$$

The formal solution to Eq. (2) for the gravitational field $U_G(\vec{r})$, with (1) as a source, is given by the integral representation

$$U_G(\vec{r}) = -G \int_{\mathbb{R}^3} \frac{\rho_M(\vec{r}\,')}{|\vec{r} - \vec{r}\,'|} dV'. \quad (3)$$

The solution (3) for the case of a homogeneous solid sphere, in principle, a six-dimensional integral, can be simplified to a three-dimensional integral over the center-of-mass coordinates as

$$U_G(\vec{r}) = \int_{\mathbb{R}^3} V_G(|\vec{r} - \vec{r}\,'|)|\Psi(\vec{r}\,')|^2 dV'. \quad (4)$$

The integral kernel $V_G(|\vec{r} - \vec{r}\,'|)$ can be interpreted as the gravitational potential at the position $\vec{r}$ due to a mass distribution centered at the position $\vec{r}\,'$. A homogeneous solid sphere has a constant density within a radius R and the integration kernel at a radial distance $r = |\vec{r}|$ from the center has been calculated analytically [20,25] and is given by

$$V_G(r) = \begin{cases} -\frac{GM^2}{R}\left[\frac{6}{5} - 2\left(\frac{r}{2R}\right)^2 + \frac{3}{2}\left(\frac{r}{2R}\right)^3 - \frac{1}{5}\left(\frac{r}{2R}\right)^5\right] & \text{if } \frac{r}{2R} \leqslant 1 \\ -\frac{GM^2}{r} & \text{if } \frac{r}{2R} > 1 \end{cases} \quad (5)$$

For distances outside $2R$, the kernel is identical to the potential due to a pointlike distribution, whereas inside $2R$, the spherical symmetry leads to shielding of the exterior fraction of the mass. As a result, only the internal mass fraction will contribute, leading to an approximately parabolic dependence of the potential for small distances of the effective potential. For intermediate distances there is a transition zone joining the two regimes in a smooth manner, thus interpolating between the behavior of a pointlike and that of an extended distribution.

Using the effective gravitational potential in Eq. (4), the center-of-mass wave function of a charge-neutral solid sphere under the influence of the Newtonian gravitational potential produced by the density $\rho_M(\vec{r})$ is governed by the time-dependent integro-differential equation

$$i\hbar \frac{\partial \Psi(\vec{r})}{\partial t} = -\frac{\hbar^2}{2M}\nabla^2 \Psi(\vec{r}) + \int_{\mathbb{R}^3} V_G(\vec{r} - \vec{r}\,')|\Psi(\vec{r}\,')|^2 dV' + V_B(\vec{r})\Psi(\vec{r}), \quad (6)$$

where $V_B(\vec{r})$ is an arbitrary external potential. Equation (6) is known as the Newton-Schrödinger equation, here written down for the case of a spatially extended mass and with an external potential added. Separation into the time-independent case is straightforward and can be done in the usual manner. The gravitational interaction term in Eq. (6) leads to bound states even for free particles, i.e., in the absence of any trapping potential. The dependence on mass and density of these free-space bound states was investigated in a previous study [24]. For high masses the quantum state is largely determined by the quadratic part of the potential, whereas for low masses the behavior is well approximated by that of a single pointlike particle [26]. In the latter case the extent of the wave function is much larger than the material distribution, which then effectively is that of a point source. A crossover between the two regimes is found at approximately 2×10^{-17} kg.

III. METHOD

With the framework presented in the preceding section in place, the next step is to solve Eq. (6), which is a nonlinear integro-differential equation with no presently known exact analytical solutions, and there are few reasons for believing that any will exist. All solutions are obtained by solving Eq. (6) with the gravitational potential (5) in the integral kernel, by either analytical approximations or numerical methods. Here I perform a numerical solution where the derivatives are calculated using a pseudospectral method [27,28]. The wave function is then computed in a discrete number of points with positions determined by the explicit choice of pseudospectral basis. We have for the two-dimensional cylindrically symmetric case we consider here

$$\Psi_{ij} = \Psi(r_i, z_j), \quad (7)$$

where r_i and z_i are the collocation points with indices

$$1 \leqslant i \leqslant N_r, \quad 1 \leqslant j \leqslant N_z. \quad (8)$$

Calculating derivatives of the wave function amounts to performing a linear transformation on the discretized wave function according to

$$\frac{\partial \Psi_{ij}}{\partial r} \approx \sum_{i'=1}^{N_r} d_{ii'} \Psi_{i'j}, \quad (9)$$

where the transformation coefficients $d_{i,j}$ are matrix elements of a pseudospectral differentiation matrix [28], which in general is dense. Higher-order derivatives as well as mappings for the other spatial variable are done in the same way. In

addition, we have to deal with the effective interaction term given by Eq. (4), where the integral can be calculated using Gaussian integration [29]

$$U_G(r_i,z_i)=\sum_{i'=1}^{N_r}\sum_{j'=1}^{N_z}V_G(r_{i'},r_i,z_{j'},z_j)|\Psi_{i'j'}|^2 w_{r,i'}w_{z,j'}, \quad (10)$$

where $w_{r,i'}$ and $w_{z,j'}$ are the Gaussian integration weights for each spatial dimension. The pseudospectral method implemented with differentiation matrices taken together with Gaussian integration represents the union of two methods that both allow for exponential convergence with respect to the basis size, which in turn guarantees high accuracy for the calculation of the quantities of interest. As it stands, the space-continuous wave function is now discretized and the time-dependent integro-differential equation (6) is transformed into a set of nonlinear ordinary differential equations

$$i\hbar\frac{\partial\Psi_{ij}}{\partial t}=H_{ij}([\Psi_{i'j'}]), \quad (11)$$

where the matrix-valued function H denotes the right-hand side of Eq. (6), which is a nonlocal function of the wave function, here denoted by the whole set of values $[\Psi_{i',j'}]$. To obtain the ground state of the system, imaginary-time propagation [30–32] can be used. The method consists in mapping the time variable into imaginary time by

$$it=\tau, \quad (12)$$

which then transforms the time-dependent set of coupled equations (11) into

$$\hbar\frac{\partial\Psi_{ij}}{\partial\tau}=-H_{ij}([\Psi_{i'j'}]), \quad (13)$$

which is of diffusion type. As a result, eigenstates decay exponentially with rates depending on the energy eigenvalues of the right-hand side of Eq. (11) As the transformation into imaginary time turns Schrödinger equations into diffusionlike differential equations, the norm decays with propagated time and the wave function must be renormalized between iterations. The resulting equations are propagated stepwise in time until convergence is reached. Demands for precision were set by the requirement that for a free-space system, the lowest energy obtained by solving the two-dimensional problem using the method here coincided with a one-dimensional method based on straightforward diagonalization and iteration up to a sufficient accuracy. The nonlinear integro-differential equation (6) is thus propagated to convergence, using a combination of pseudospectral collocation and mapping onto imaginary time, with the method of lines [33].

IV. RESULTS

As the first investigation, the ground-state energy was determined using Eq. (6) by solving the equation numerically until convergence was reached, followed by repeating the procedure for different values of the mass. In Fig. 1 the ground-state energy for a sphere of fused silica is shown as a function of total mass. For low masses, the system becomes weakly bound, which is seen as a change in the slope of the ground-state energy as a function of mass. Also shown in Fig. 1 is $V_G(0)$,

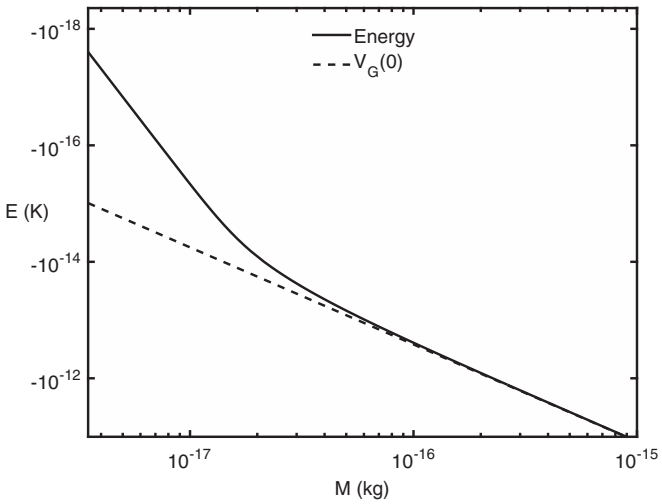

FIG. 1. Ground-state energy as a function of mass for a self-gravitating quantum sphere of fused silica in the absence of any confining potential. The dotted line shows the bottom of the bare gravitational potential $V_G(0)$ given by Eq. (5). For large masses the ground state becomes strongly bound and is located close to the bottom of the bare potential, as can be seen in the figure. For small masses the system is weakly bound and a crossover between the two behaviors can be seen at $M\approx 2\times 10^{-17}$ kg. This latter value of the mass gives rise to a state with average radius of the center-of-mass wave function comparable to that of the solid mass distribution.

the bottom of the bare potential given by Eq. (5). For high masses, the ground-state energy is close to the bottom, whereas for low masses it rapidly approaches zero. The weakly bound states are spread out outside R, the radius of the bulk sphere, and as a result the gravitational interaction becomes averaged over a large region, resulting in a weak effective potential. The gravitational interaction is then too weak to localize the free-space quantum state enough for it to experience the inner part of the effective potential sufficiently to become more deeply bound. Averaging the self-interaction term over the wave function thus effectively makes the potential shallower for extended states.

In principle, there is also a dependence of $U_G(\vec{r})$ on the density, which is often fairly weak and which becomes negligible for sufficiently low masses where the size of the solid sphere is irrelevant. A solid sphere of radius R and density ϱ has a mass $M=4\pi\varrho R^3/3$, where the density of solid elements varies from $\varrho=534\ \mathrm{kg\,m^{-3}}$ for lithium to $\varrho=22\,610\ \mathrm{kg\,m^{-3}}$ for osmium, the densest stable element. Here I use the density of fused silica, $\varrho=2210\ \mathrm{kg\,m^{-3}}$, as this material has been used in experiments both for the cooling of the center-of-mass motion in optical traps [34] and also for suggestions of experiments probing the quantum-classical boundary [9].

Noting that the interior of the effective potential constitutes a potential well of finite depth, it begs the question as to whether or not the wave function can be made to probe its bottom by any external manipulation. It turns out that increased localization can be produced with the addition of a trapping potential, which in turn could lead to a lowering of the ground-state energy. A similar shift in energy happens with Bose-Einstein condensates [35] with negative scattering

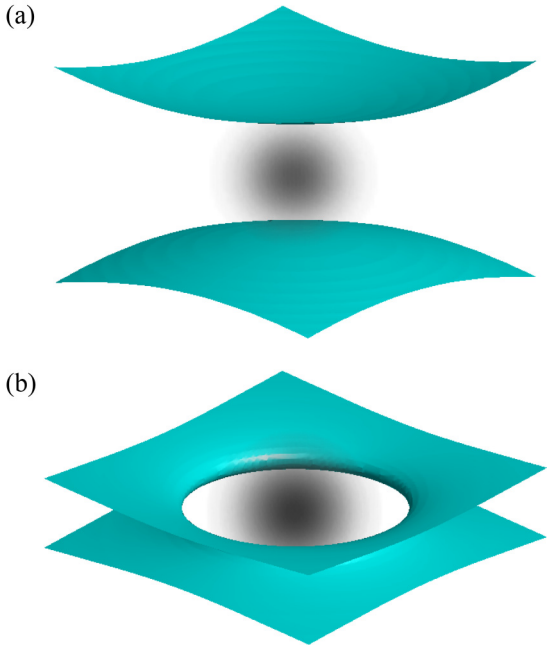

FIG. 2. Picture of ground-state wave functions and equipotential surfaces for two potential configurations that lower the energy: (a) a vertical confinement configuration, as given by Eq. (14), and (b) the radial confinement configuration given by Eq. (15).

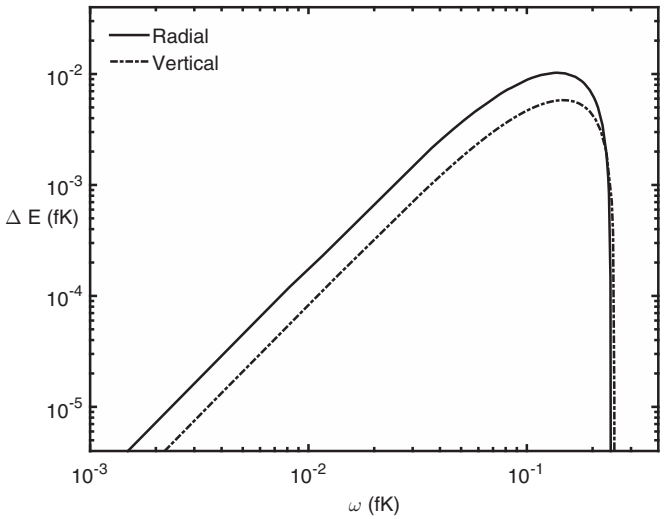

FIG. 3. Lowering of the ground-state energy for potentials with radial confinement (dash-dotted line) of the form given by Eq. (15) and also for vertical confinement (solid line) as given by Eq. (14).

lengths. In straightforward terms, the effect of a closed trapping potential can be seen to increase the spatial localization and thus enhance the effect due to the gravitational self-interaction term, effectively lowering the ground-state energy. In quantum mechanics, on the other hand, such regions in space, where potential surfaces have saddle points, are dynamically avoided since the quantum pressure will always produce an effective force resulting in repulsion away from narrow regions. With the gravitational interaction the situation is different as an attractive nonlinearity can balance and even contribute more than the increased repulsion due to the quantum pressure. Here I present examples of potentials where the presence of saddle points leads to a lowering of the ground-state energy through increased localization. To investigate the behavior in some detail, two different potential functions were used. Both were chosen to be open and to have minima equaling zero at the origin. As a result, these potentials do not support bound states without the presence of the gravitational term in the Hamiltonian. For the sake of simplicity, only systems with cylindrical symmetry were used as this reduces the numerical complexity of the calculations. The first system, which consists of an axially symmetric harmonic binding in the z direction, has a potential given by

$$V_B(\vec{r}) = \frac{M\omega_z^2}{2} z^2 e^{-r^2/2\Delta z^2}, \tag{14}$$

where ω_z is the transverse oscillator frequency at the center of the potential. Here the value $M = 1 \times 10^{-17}$ kg is used as this is right at the boundary of the delocalized regime, yet is large enough to give a fairly localized state. A contour surface for the potential is shown in Fig. 2(a) together with the resulting probability density as a shaded cloud for the center-of-mass wave function. The potential becomes less confined with increasing radial distance approaching zero far from the z axis. The second potential, shown in Fig. 2(b), is given by

$$V_B(\vec{r}) = \frac{M\omega_r^2}{2} r^2 e^{-z^2/2\Delta z^2}, \tag{15}$$

where ω_r is the transverse oscillator frequency at the center of the potential. This potential has a central narrowing reminiscent of a quantum point contact [36–38]. For both potentials (14) and (15) the numerical solutions showed that the wave function localizes to the center of the potential despite the fact that the quantum pressure is higher there as both of the potentials have their narrowest regions at the origin. The increased attraction from the gravitational interaction thus wins over the increase in quantum pressure due to the repulsion from the external potential. Lowering of the ground-state energy of the system locally indicates that a quantum system will seek these regions as they are energetically favorable. For both potentials, the transverse binding strengths, as measured by the transverse oscillator frequencies ω_r and ω_z, were varied and the resulting equation was solved to determine the magnitude of the lowering of the ground-state energy. The energy shift was calculated as

$$\Delta E = E - E_0, \tag{16}$$

where E_0 is the ground-state energy without the potential. The energy shifts are shown in Fig. 3 as functions of the transverse oscillator frequency for both cases of trapping. Both energy shifts were found to increase quadratically with the transverse oscillator frequencies. This can be expected from perturbation theory, which applies when the trapping is sufficiently weak, corresponding to the oscillator frequency being small enough. As can be seen in Fig. 3, the initial slopes for $\Delta E(\omega)$ are identical. For larger values of trapping frequencies, maxima are reached, beyond which it no longer pays to increase the strength and the energy shifts go through a zero. For larger values of the oscillator frequency, the gravitational interaction

no longer dominates the change in ground-state energy and the state is no longer preferable over the free-space solution. There is thus a limited parameter region for both cases of trapping where the state will localize at the origin due to lowering of the ground-state energy.

V. DISCUSSION

In this study I have presented a nontrivial quantum feature of self-gravitating solid systems in the presence of external potentials, namely, the lowering of ground-state energy at the center of unstable potentials. It follows readily that sufficiently cold nanospheres will be trapped at the potential centers despite the possibly unstable character of the latter. The reason why a repulsive potential can lower the ground-state energy of a self-gravitating quantum system is that the potential induces a change in the balance between quantum pressure, i.e., curvature of the wave function, and the self-gravitational attraction. The repulsive potential will lower the density in the region where the potential is high and as a result the density will become higher at the center of the state. This change to the center-of-mass wave function reduces the averaging of the interaction term and results in a deeper effective potential. This mechanism will lower the ground-state energy as long as there is a net gain in the changed balance between the different contributions to the energy. Since the gravitational potential is bounded from below, there is a limit on how much energy can be gained and eventually quantum pressure wins out, increasing the energy if the compression becomes too large. The presence of a self-gravitating system in the vicinity of two different potential surfaces can, in principle, lower the energy as a function of interpotential distance and would give rise to an effective force between different potential surfaces. This constitutes a force of quantum-mechanical origin, similar in this sense to the Casimir-Polder force [39,40], which is due to zero-point fluctuations in a quantum field. The potential given by Eq. (14) and shown in Fig. 2(a) is similar in shape to the configuration used for quantum point contacts [36] in that it has a narrowing, although in three dimensions rather than in two. In quantum point contacts, it has been suggested that the presence of a bound state due to effective spin-spin interactions could provide an explanation for the 0.7 conductance anomaly [41]. Here we thus have an analogous situation inducing a nontrivial result for an interacting system in a constriction. In both cases the interaction leads to a localized quantum state defying classical expectations for the system. We also note that Bose-Einstein condensates with attractive interaction, i.e., negative scattering length, have bound states with increased localization, but that these are limited in terms of the number of atoms that can be included since there is no lower bound on the interaction energy. A similar effect should thus be observable for attractive Bose-Einstein condensates of small particle numbers.

Experiments in cooling objects [34], either in liquids or trapped in optical lattices, and measuring forces on them have reached sensitivities of femtonewtons [42] and zeptonewtons [43] respectively, showing the considerable progress being done in detecting weak influences on objects, especially in the quantum regime. The energy shifts involved in the effects studied here are exceedingly small, corresponding to temperatures around femtokelvin degrees or less due to the feebleness of gravity. The lowest temperature achieved experimentally so far is around 500 fK for Bose-Einstein condensates [44] and microkelvin degrees for solids [45]. Observation of these effects in the quantum regime will thus require further developments in the cooling of solid objects [46,47]. In addition, the presence of environmental decoherence will make it challenging to observe these effect, especially due to scattering if optical potentials are used. It is thus most likely that these effects will require experiments in low gravity. Present experiments are conducted in the microgravity of a drop tower [48], as well as in airborne zero-gravity environments [49]. In the near future, space-borne missions [50–52] will reach noise levels on the order of femtokelvin degrees. To go to temperatures below this, shielding of gravitational noise must be done and passive noise attenuation will reach down to picogravity [53], which will be insufficient for measuring the shifts discussed here, indicating the need for further developments.

ACKNOWLEDGMENTS

The computations were performed on resources provided by the Swedish National Infrastructure for Computing through Uppsala Multidisciplinary Center for Advanced Computational Science under Project No. SNIC p2013046.

[1] M. Albers, C. Kiefer, and M. Reginatto, Phys. Rev. D **78**, 064051 (2008).
[2] C. Kiefer, *Quantum Gravity* (Oxford University Press, Oxford, 2012).
[3] C. Rovelli, *Quantum Gravity* (Cambridge University Press, Cambridge, 2004).
[4] H. Rauch and S. A. Werner, *Neutron Interferometry: Lessons in Experimental Quantum Mechanics, Wave-Particle Duality, and Entanglement* (Oxford University Press, Oxford, 2015).
[5] V. V. Nezvizhevsky *et al.*, Nature (London) **415**, 297 (2002).
[6] C. G. Aminoff, A. M. Steane, P. Bouyer, P. Desbiolles, J. Dalibard, and C. Cohen-Tannoudji, Phys. Rev. Lett. **71**, 3083 (1993).
[7] T. Kovachy, P. Asenbaum, C. Overstreet, C. A. Donnelly, S. M. Dickerson, A. Sugarbaker, J. M. Hogan, and M. A. Kasevich, Nature (London) **528**, 530 (2015).
[8] M. Aspelmeyer, T. Kippenberg, and F. Marquardt, Rev. Mod. Phys. **86**, 1391 (2014).
[9] D. E. Chang, C. A. Regal, S. B. Papp, D. J. Wilson, J. Yeb, O. Painter, H. J. Kimbleb, and P. Zoller, Proc. Natl. Acad. Sci. U.S.A. **107**, 1005 (2010).
[10] W. Marshall, C. Simon, R. Penrose, and D. Bouwmeester, Phys. Rev. Lett. **91**, 130401 (2003).
[11] O. Romero-Isart, M. L. Juan, R. Quidant, and J. I. Cirac, New J. Phys. **12**, 033015 (2010).

[12] E. Joos, H. D. Zeh, C. Kiefer, D. J. W. Giulini, J. Kupsch, and I.-O. Stamatescu, *Decoherence and the Appearance of a Classical World in Quantum Theory* (Springer, Heidelberg, 2003).
[13] L. Diosi, Phys. Lett. A **105**, 199 (1984).
[14] R. Penrose, Philos. Trans. R. Soc. A **356**, 1743 (1998).
[15] R. Ruffini and S. Bonazzola, Phys. Rev. **187**, 1767 (1969).
[16] C. Lämmerzahl, Appl. Phys. B **84**, 551 (2006).
[17] M. Jääskeläinen, Found. Phys. **45**, 591 (2015).
[18] S. L. Adler, J. Phys. A **40**, 755 (2007).
[19] C. Anastopoulos and B. L. Hu, New. J. Phys. **16**, 085007 (2014).
[20] S. Colin, T. Durt, and R. Willox, Class. Quantum Grav. **31**, 245003 (2014).
[21] A. Großardt, J. Bateman, H. Ulbricht, and A. Bassi, Sci. Rep. **6**, 30840 (2016).
[22] H. Yang, H. Miao, D. S. Lee, B. Helou, and Y. Chen, Phys. Rev. Lett. **110**, 170401 (2013).
[23] M. Bahrami, A. Großardt, S. Donadi, and A. Bassi, New J. Phys. **16**, 115007 (2014).
[24] M. Jääskeläinen, Phys. Rev. A **86**, 052105 (2012).
[25] F. Carstoiu and R. J. Lombard, Ann. Phys. (N.Y.) **217**, 279 (1992).
[26] I. Moroz, R. Penrose, and P. Tod, Class. Quantum Grav. **15**, 2733 (1998).
[27] B. Fornberg, *A Practical Guide to Pseudospectral Methods* (Cambridge University Press, Cambridge, 1998).
[28] J. A. C. Weideman and S. C. Reddy, ACM Trans. Math. Software **26**, 465 (2000).
[29] P. K. Kythe and M. R. Schäferkotter, *Handbook of Computational Methods for Integration* (Chapman and Hall/CRC, Boca Raton, 2005).
[30] G. A. Baker Jr., J. L. Gammel, B. J. Hill, and J. G. Wills, Phys. Rev. **125**, 1754 (1962).
[31] A. Goldberg and J. L. Schwartz, J. Comput. Phys. **1**, 433 (1967).
[32] A. Goldberg and J. L. Schwartz, J. Comput. Phys. **1**, 448 (1967).
[33] W. E. Schiesser, *The Numerical Method of Lines: Integration of Partial Differential Equations* (Academic, San Diego, 1991).
[34] T. Li, S. Kheifets, and M. G. Raizen, Nat. Phys. **7**, 527 (2011).
[35] C. J. Pethick and H. Smith, *Bose-Einstein Condensation in Dilute Gases* (Cambridge University Press, Cambridge, 2010).
[36] H. van Houten and C. W. J. Beenakker, Phys. Today **49** (7), 22 (1996).
[37] B. J. van Wees, H. van Houten, C. W. J. Beenakker, J. G. Williamson, L. P. Kouwenhoven, D. van der Marel, and C. T. Foxon, Phys. Rev. Lett. **60**, 848 (1988).
[38] D. A. Wharam, *et al.*, J. Phys. C **21**, L209 (1988).
[39] H. B. G. Casimir, Proc. K. Ned. Akad. Wet. B **51**, 793 (1948).
[40] H. B. G. Casimir and D. Polder, Phys. Rev. **73**, 360 (1948).
[41] T. Rejec and Y. Meir, Nature (London) **442**, 900 (2006).
[42] L. Liu, S. Kheifets, V. Ginis, and F. Capasso, Phys. Rev. Lett. **116**, 228001 (2016).
[43] G. Ranjit, M. Cunningham, K. Casey, and A. A. Geraci, Phys. Rev. A **93**, 053801 (2016).
[44] A. E. Leanhardt, T. A. Pasquini, M. Saba, A. Schirotzek, Y. Shin, D. Kielpinski, D. E. Pritchard, and K. Ketterle, Science **301**, 1513 (2003).
[45] V. Jain, J. Gieseler, C. Moritz, C. Dellago, R. Quidant, and L. Novotny, Phys. Rev. Lett. **116**, 243601 (2016).
[46] D. V. Seletskiy, R. Epstein, and M. Sheik-Bahae, Rep. Prog. Phys. **79**, 096401 (2016).
[47] O. M. Marago, P. H. Jones, P. G. Gucciardi, G. Volpe, and A. C. Ferrari, Nat. Nanotech. **8**, 807 (2013).
[48] T. van Zoest *et al.*, Science **328**, 1540 (2010).
[49] R. Geiger *et al.*, Nat. Commun. **2**, 474 (2011).
[50] R. Kaltenbaek *et al.*, EPJ Quantum Technol. **3**, 5 (2016).
[51] R. Kaltenbaek, G. Hechenblaikner, N. Kiesel, W. Wieczorek, S. Hofer, S. Gröblacher, M. R. Vanner, F. Blaser, U. Johann, and M. Aspelmeyer, Macroscopic quantum experiments in space (MQES), European Space Agency Report, 2012 (unpublished).
[52] Scientific perspectives for ESA's future programme in life and physical sciences in space, European Science Foundation report, 2007 (unpublished).
[53] G. Catastini, D. Bramanti, A. M. Nobili, F. Fuligni, and V. Iafolla, ESA J. **16**, 401 (1992).